coefficient by rank test.

RESULTS

Clinical Manifestations

A total of nine men and two women ranging in age from 23 to 71 years (mean age: 60.6 years) were enrolled in the study. No abnormalities were found for the systemic investigations and laboratory tests. Serology examinations for human immunodeficiency virus were all negative. None of the patients had any history of eye surgery prior to the onset of uveitis. Clinical findings of the CMV-associated iridocyclitis patients (n=7) and corneal endotheliitis patients (n=4) are shown in Table 1. A unilateral mild anterior uveitis with high IOP was noted in all 11 patients. There were no significant differences between the iridocyclitis and corneal endotheliitis groups for the cells and flare values in the anterior chamber, nor were there any differences noted for the elevated levels of IOP, KPs, gonioscopic findings, and iris atrophy. Stromal edema of the cornea was seen in all corneal endotheliitis but not in iridocyclitis patients. While the stromal edema was diffuse in three out of the four patients, it was localized at upper cornea in one of the corneal endotheliitis patients. Representative cases for iridocyclitis and corneal endotheliitis are shown in Figs. 1 and 2, respectively. As for the IOP elevation, all 11 eyes required anti-glaucoma medications, with two eyes (cases 1 and 2) requiring trabeculectomy. With regard to the iris atrophy, no sectorial iris atrophy was seen in all 11 eyes, although four eyes (two each in the iridocyclitis and the corneal endotheliitis groups, respectively) presented diffuse iris atrophy.

Systemic valganciclovir therapy (1800 mg/day for longer than 3 weeks) in conjunction with topical corticosteroids and anti-glaucoma agents effectively controlled the inflammation

in the anterior segment of the eye as well as the high IOP.

Corneal Endothelial Cell Loss

Specular microscopic examination revealed significant corneal endothelial cell loss (35% or more) in all 11 patients (Table 2). Severe corneal endothelial cell loss larger than 70% was recorded in more than half of the endotheliitis group eyes. In contrast, this severe cell loss was observed in one of the seven patients with iridocyclitis.

There are several patients (case 1, 8, 10, and 11 in Table 2) with corneal endothelial cell counts less than 700 cells/mm^2. Among the patients, three cases had a low visual acuity between 0.3 and 0.6. However, one patient had a good visual acuity of 1.5.

PCR Analysis of the Aqueous Humor Samples

Multiplex PCR analyses confirmed the presence of CMV genomic DNA, but not any of the other human herpes viruses (HSV-1, HSV-2, VZV, EBV, HHV-6, HHV-7 or HHV-8), in all 11 of the patients (Table 2).

Quantitative real-time PCR detected significant viral loads of CMV genomic DNA in the aqueous humor of all 11 patients, with values ranging from 5.4×10^3 to 5.9×10^6 copies/ml (Table 2). The mean values for the CMV viral load in the iridocyclitis and corneal endotheliitis groups were 9.4×10^5 and 1.2×10^6 copies/ml, respectively. The differences in CMV viral load between the two groups were not significant ($P = 0.571$).

The corneal endothelial cell damage intensity was correlated to the CMV viral load in the aqueous humor. Results of the linear regression analysis demonstrated a positive correlation between the CMV viral load and the corneal endothelial cell loss (Spearman's correlation coefficient by rank test, r = 0.664; $P = 0.036$; Fig. 3).

However, there was no correlation between the interval from the disease onset to the aqueous sampling and the viral load in the aqueous humor (Spearman's correlation coefficient by rank test, r = 0.445; P = 0.159). Furthermore, the interval from the disease onset to the sampling was not correlated with the corneal endothelial cell damage intensity (Spearman's correlation coefficient by rank test, r = 0.373; P = 0.239). In addition, there was also no correlation between the viral load and many other ocular findings, such as cells and flare in the anterior chamber, types of KPs, gonioscopic findings, IOP, and post-treatment BCVA.

DISCUSSION

The present study analyzed ocular manifestations and CMV viral loads in the aqueous humor of patients with CMV-associated iridocyclitis and corneal endotheliitis. Our major findings included: (1) presence of significant corneal endothelial cell loss in both corneal endotheliitis and iridocyclitis tested eyes, and (2) a significant correlation between corneal endothelial cell loss and CMV viral load in the aqueous humor.

Even though it has been demonstrated that viral infections play a significant role in many inflammatory diseases, a qualitative PCR method that is capable of determining the pathologic role of these viral infections has yet to be elucidated. If the presence of viral DNA in an affected disease site could be proven, the quantitative determination and correlation to the clinical manifestations of the viral infection could lead to a much deeper understanding of the role of the virus as a pathogenic disease candidate. For example, we have previously reported on two intraocular inflammatory disorders: one involving uveitis associated with human T-cell leukemia virus type 1 (HTLV-1) [13, 14] and the other involving anterior uveitis associated with VZV [14]. In HTLV-1 uveitis, a significantly higher HTLV-1 viral load was detected in

the peripheral blood mononuclear cells of the patients when compared to asymptomatic HTLV-1 carriers [13]. This viral load was significantly correlated with the vitreous inflammation of the disease [14]. In our report on anterior uveitis associated with VZV, we demonstrated there was a high VZV viral load within the patient's aqueous humor. Furthermore, there was a significant correlation between the viral load and the intensity of the iris atrophy in these patients [15].

Although we found that there was a positive correlation between the corneal endothelial cell loss and the CMV viral load in the aqueous humor, there was no correlation between the viral load and many other ocular signs such as cells and flare in the anterior chamber, types of KPs, gonioscopic findings, IOP, post-treatment visual acuity, and the interval from the disease onset to the aqueous sampling. These patients had been treated with topical corticosteroids (e.g., betamethasone) and anti-glaucoma agents (e.g., timolol and latanoprost) before they were referred to us by local ophthalmologists. These treatments are known to reduce the intensity of anterior uveitis, IOP and other ocular manifestations, but have no effects on recovering the corneal endothelial cell damage, because the corneal endothelial cell damage is well known to hardly to recover once it occurs.

The cells and flare in the anterior chamber are mild in all 11 patients. A possible explanation why the intensity of the inflammatory reaction in the anterior chamber is so mild in this disease might be related to the involvement of the anterior chamber-associated immune deviation (ACAID) [16, 17]. In an experimental rabbit corneal endotheliitis model, eyes inoculated with inactivated HSV-1 prior to an active HSV-1 infection exhibited less severe inflammatory reactions and corneal endotheliitis. In addition, they also developed an immune deviation to HSV-1 [18]. Although CMV-related ACAID has not been previously reported, real-time PCR in the present study demonstrated that genomic DNA of CMV was present at

high levels within the anterior chamber of the patients. Therefore, it may very well be that ACAID in response to CMV could possibly occur in the eye, resulting in a relatively mild inflammatory reaction.

While our results showed CMV infection in the anterior segment of the eye caused inflammation and corneal endothelial cells loss in immunocompetent hosts, our study cannot answer many other questions. For example, why does CMV cause intraocular inflammation in immunocompetent hosts? Where does the CMV that is detected in the aqueous humor come from? And, how is CMV able to cause inflammatory disorder only within the anterior segment of the eye? One possible explanation why our patients developed CMV anterior uveitis is that all our patients had been given topical corticosteroids for a long period. This may attributed to induce local immunosuppressive condition in the anterior segment of the eye and to result in reactivation of CMV [19]. Further clinical and experimental investigations are necessary to clarify these important questions.

In conclusion, significant corneal endothelial cell damage was detected in all CMV-associated iridocyclitis and corneal endotheliitis tested eyes. In addition, a significant correlation was found between corneal endothelial cell loss and the CMV viral load in the aqueous humor.

Funding: None.

Competing interests: None.

Ethics approval: Ethics approval was provided by the Institutional Ethics Committee of Tokyo Medical and Dental University.

Patient consent: Obtained.

FIGURE LEGENDS

Figure 1. Case 4: Slit-lamp microscopy photo with CMV-associated iridocyclitis.

Mutton fat keratic precipitates with some pigmentation were scattered within the central area of the cornea. There was mild inflammation found within the anterior chamber.

Figure 2. Case 8: Slit-lamp microscopy photo with CMV-associated corneal endotheliitis.

Diffuse corneal stromal edema with folds in Descemet's membrane was observed.

Figure 3. Correlation between CMV viral load and corneal endothelial cell damage.

The CMV viral load was plotted on a logarithmic graph versus the % corneal endothelial cell loss. The scatterplot shows significant correlation between the CMV viral load and the % corneal endothelial cell loss (Spearman's correlation coefficient by rank test, r = 0.664; P = 0.036).

REFERENCES

1. Yoser SL, Forster DJ, Rao NA. Systemic viral infections and their retinal and choroidal manifestations. *Surv Ophthalmol* 1993;**37**:313-352.
2. Mietz H, Aisenbrey S, Ulrich Bartz-Schmidt K, et al. Ganciclovir for the treatment of anterior uveitis. *Graefes Arch Clin Exp Ophthalmol* 2000;**238**:905-909.
3. Markomichelakis NN, Canakis C, Zafirakis P, et al. Cytomegalovirus as a cause of anterior uveitis with sectoral iris atrophy. *Ophthalmology* 2002;**109**:879-882.
4. de Schryver I, Rozenberg F, Cassoux N, et al. Diagnosis and treatment of cytomegalovirus iridocyclitis without retinal necrosis. *Br J Ophthalmol* 2006;**90**:852-855.
5. Chee SP, Jap A. Presumed fuchs heterochromic iridocyclitis and Posner-Schlossman syndrome: comparison of cytomegalovirus-positive and negative eyes. *Am J Ophthalmol* 2008;**146**:883-889.
6. Kawaguchi T, Sugita S, Shimizu N, et al. Kinetics of aqueous flare, intraocular pressure and virus-DNA copies in a patient with cytomegalovirus iridocyclitis without retinitis. *Int Ophthalmol* 2007;**27**:383-386.
7. Koizumi N, Yamasaki K, Kawasaki S, et al. Cytomegalovirus in aqueous humor from an eye with corneal endotheliitis. *Am J Ophthalmol* 2006;**141**:564-565.
8. Chee SP, Bacsal K, Jap A, et al. Corneal endotheliitis associated with evidence of cytomegalovirus infection. *Ophthalmology* 2007;**114**:798-803.
9. Koizumi N, Suzuki T, Uno T, et al. Cytomegalovirus as an etiologic factor in corneal endotheliitis. *Ophthalmology* 2008;**115**:292-297.
10. Sugita S, Shimizu N, Kawaguchi T, et al. Identification of human herpes virus 6 in a patient with severe unilateral panuveitis. *Arch Ophthalmol* 2007;**125**:1426–1427.
11. Sugita S, Shimizu N, Watanabe K, et al. Use of multiplex PCR and real-time PCR to detect

human herpes virus genome in ocular fluids of patients with uveitis. *Br J Ophthalmol* 2008;**92**:928-932.

12. Schaade L, Kockelkorn P, Ritter K, et al. Detection of cytomegalovirus DNA in human specimens by LightCycler PCR. *J Clin Microbiol* 2000;**38**:4006-4009.
13. Ono A, Mochizuki M, Yamaguchi K, et al. Increased number of circulating HTLV-1 infected cells in peripheral blood mononuclear cells of HTLV-1 uveitis patients: a quantitative polymerase chain reaction study. *Br J Ophthalmol* 1995;**79**:270-276.
14. Ono A, Mochizuki M, Yamaguchi K, et al. Immunologic and virologic characterization of the primary infiltrating cells in the aqueous humor of human T-cell leukemia virus type-1 uveitis. Accumulation of the human T-cell leukemia virus type-1-infected cells and constitutive expression of viral and interleukin-6 messenger ribonucleic acids. *Invest Ophthalmol Vis Sci* 1997;**38**:676-689.
15. Kido S, Sugita S, Horie S, et al. Association of varicella zoster virus load in the aqueous humor with clinical manifestations of anterior uveitis in herpes zoster ophthalmicus and zoster sine herpete. *Br J Ophthalmol* 2008;**92**:505-508.
16. Streilein JW, Wilbanks GA, Taylor A, et al. Eye-derived cytokines and the immunosuppressive intraocular microenvironment: a review. *Curr Eye Res* 1992;**11 Suppl**:41-47.
17. Streilein JW. Ocular immune privilege and the Faustian dilemma. The Proctor lecture. *Invest Ophthalmol Vis Sci* 1996;**37**:1940-1950.
18. Zheng X, Yamaguchi M, Goto T, et al. Experimental corneal endotheliitis in rabbit. *Invest Ophthalmol Vis Sci* 2000;**41**:377-385.
19. Chee SP, Bacsal K, Jap A, et al. Corneal endotheliitis associated with evidence of cytomegalovirus infection. *Ophthalmology* 2007;**114**:798-803.

Table 1. Clinical findings in patients with CMV anterior uveitis

Case	Age (years)	Sex	Eye	Diagnosis	Corneal edema	KPs	Cells in AC	Flare in AC	IOP (mmHg)	Pigmentation in the AC angle	Iris atrophy
1	66	M	R	Iridocyclitis	-	Mutton-fat	1+	17	38	Depigmentation	None
2	62	M	R	Iridocyclitis	-	Mutton-fat	1+	26	40	PAS & pigment	Diffuse
3	56	M	L	Iridocyclitis	-	Mutton-fat	1+	13	44	Depigmentation	Diffuse
4	53	F	R	Iridocyclitis	-	Mutton-fat	1+	13	36	Depigmentation	None
5	71	M	L	Iridocyclitis	-	Mutton-fat	2+	28	25	PAS	None
6	63	M	R	Iridocyclitis	-	Fine	1+	Nt	50	Depigmentation	None
7	23	M	R	Iridocyclitis	-	Fine	1+	Nt	25	Depigmentation	None
8	71	M	R	Endotheliitis	+ (diffuse)	Mutton-fat	2+	151	37	PAS	None
9	67	M	R	Endotheliitis	+ (diffuse)	Fine	1+	14	25	Depigmentation	Diffuse
10	64	F	L	Endotheliitis	+ (superior)	Fine	1+	21	28	Depigmentation	None
11	71	M	R	Endotheliitis	+ (diffuse)	Mutton-fat	1+	12	43	PAS	Diffuse

Information of 11 patients with CMV anterior uveitis was reviewed. Data collected included intraocular pressure (IOP) and clinical manifestation of the anterior segments in the affected eye. M, male; F, female; KPs, keratic precipitates; AC, anterior chamber; PAS, peripheral anterior synechia; Nt, not tested.

Table 2. Virological analysis and corneal endothelial cell findings in patients with CMV anterior uveitis

Case	Herpes virus DNA		Endothelial cell count (cells/mm^2)		% Corneal endothelial cell loss **	Post-treatment BCVA	Interval from onset to sampling (months)
	CMV (copies/ml)	Others*	Affected eye	Fellow eye			
1	2.3×10^5	-	642	2738	77	0.4	96
2	5.5×10^3	-	1633	2869	43	0.8	8
3	1.3×10^4	-	1695	2789	39	1.5	48
4	6.5×10^4	-	1618	3576	55	1.5	24
5	3.5×10^5	-	1445	2608	38	1.2	14
6	5.9×10^6	-	919	2288	45	1.2	16
7	5.4×10^3	-	2512	3917	60	1.2	6
8	1.0×10^6	-	573	2427	76	0.6	12
9	2.8×10^4	-	1427	2262	35	0.7	5
10	1.2×10^4	-	593	2092	72	0.3	4
11	3.6×10^6	-	620	2674	77	1.5	20

Using aqueous humor samples, genomic DNA of the human herpes viruses was measured by qualitative multiplex PCR & quantitative real-time PCR. Corneal endothelial cell count was examined by specular microscopy. *Herpes viruses excluding CMV, i.e., herpes simplex virus type 1 and type 2, varicella zoster virus, Epstein-Barr virus, human herpes virus types 6, 7 and 8. ** % Corneal endothelial cell loss was calculated as described in the methods section. BCVA, best-corrected visual acuity (decimal fraction).

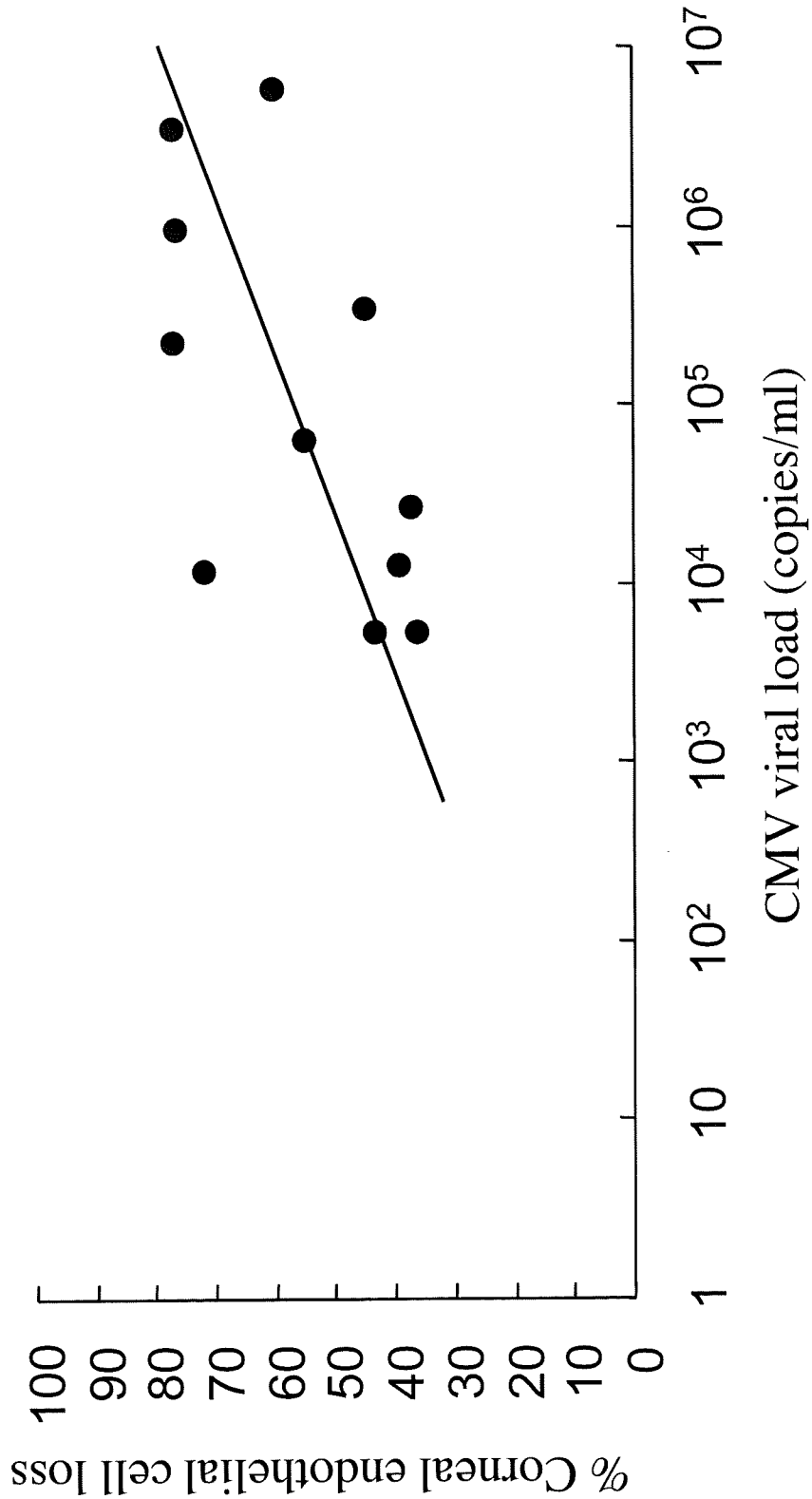

Fatal degeneration of specialized cardiac muscle associated with chronic active Epstein–Barr virus infection

Daiichiro Hasegawa,[1] Michiko Kaji,[1] Hiroki Takeda,[1] Keiichiro Kawasaki,[1] Hironobu Takahashi,[2] Hiroshi Ochiai,[3] Tomohiro Morio,[3] Yasuhiro Omori,[4] Hiroshi Yokozaki[4] and Yoshiyuki Kosaka[1]

[1]*Department of Hematology and Oncology, Kobe Children's Hospital,* [4]*Division of Pathology, Kobe University Graduate School of Medicine, Kobe,* [2]*Department of Pediatrics, Himeji Red Cross Hospital, Hyogo and* [3]*Center for Cell Therapy, Tokyo Medical and Dental University, Tokyo, Japan*

Key words ATG, CAEBV, cardiac muscle, Epstein-Barr virus, hematopoietic stem cell transplantation.

Chronic active Epstein–Barr virus infection (CAEBV) is a life-threatening disorder characterized by prolonged fever, wasting, hepatosplenomegaly, and cytopenia, in addition to abnormal EBV antibody titers and the presence of EBV antigens or EBV-DNA in tissue.[1] The ultimate prognosis of CAEBV is very poor, and patients with CAEBV often develop a progressive cellular and humoral immunodeficiency with pancytopenia and hypoglobulinemia that renders them susceptible to opportunistic infections or B- or T-cell lymphoproliferative disease.[2] An effective treatment for CAEBV has yet to be established, although allogeneic hematopoietic stem cell transplantation (HSCT) was recently reported to be effective in eradicating EBV-infected lymphocytes.[3,4] Allogeneic HSCT is, however, accompanied by a considerable risk of therapy-related death. Kimura *et al.* reported that approximately one-half of patients with CAEBV who underwent HSCT died within 60 days.[5]

We here report a patient with CAEBV who developed fatal acute circulatory failure during the preconditioning of HSCT, and in whom autopsy showed degeneration of specialized cardiac muscle and severe large-vessel arteritis associated with CAEBV.

Case report

A 12-year-old boy was admitted to a regional hospital with a 2 year history of fever, wasting, and a short stature (–3.0 SD). He was diagnosed with CAEBV on clinical signs and the presence of EBV genome in peripheral blood, and was admitted to hospital in April 2005. He was allergic to mosquito bites. On examination, lymph node adenopathy was noted. No skin lesion was observed. On brain CT, bilateral calcification of the basal ganglia was noted. Echocardiography showed dilatation of the lumens of the coronary arteries. The leukocyte count was 2.2×10^9/L; hemoglobin, 12.5 g/dL; and platelet count, 61×10^9/L. Biochemical analysis was as follows: aspartate aminotransferase, 28 IU/L; alanine aminotransferase, 14 IU/L; lactate dehydrogenase, 265 IU/L; C-reactive protein, 0.63 mg/dL; soluble interleukin-2 receptor, 1200 U/mL (normal, <519 U/mL); viral capsid antigen (VCA)-IgG, ×320; EA-IgG, ×10; EBNA, ×10. Natural killer activity was 55%. The quantity of EBV genome DNA was increased (2.6×10^3 copies/μg DNA) on polymerase chain reaction in peripheral blood mononuclear cell (PBMC), particularly in CD4+T cells (4.3×10^4 copies/μg DNA), but not in CD8+T cells or CD56+NK cells. Southern blot of the peripheral blood cells using an EBV terminal probe indicated monoclonal proliferation of EBV-infected lymphocytes. Flow cytometry showed the expression of the perforin protein in PBMC. Chromosome analysis of peripheral blood showed the normal male karyotype.

The high load of EBV genome DNA had persisted for over 6 months. Therefore, HSCT from a human leukocyte antigen (HLA)-matched sibling donor was planned in October 2005. Just before bone marrow transplantation, the quantity of EBV-DNA was consistently high in peripheral blood. No chemotherapy was performed prior to bone marrow transplantation. Echocardiography showed normal cardiac function. The exercise electrocardiogram (ECG) identified no abnormal findings.

The preparative conditioning regimen consisted of fludarabine (30 mg/m^2 × 4, day –7, –6, –5, –4), anti-thymocyte globulin (15 mg/kg × 5, day –7, –6, –5, –4, –3), and melphalan (70 mg/m^2 × 2, day –3, –2). Because anti-thymocyte globulin had been administered, he had suffered from high fever, skin rash, systemic arthralgia, and abdominal pain. He had wine-colored urine, but not microhematuria. He was diagnosed as having serum sickness and disseminated intravascular coagulation syndrome, and treated with gabexate mesilate, fresh frozen plasma, platelet transfusions, and methylprednisolone. Therefore, subsequent conditioning was all stopped on day –6 before transplantation. Blood examination showed elevation of liver enzymes, creatinine kinase, and coagulopathy. Fifty-two hours after the beginning of conditioning for transplant (on day –5), he suddenly developed acute circulatory failure. Just before cardiac arrest, echocardiogram showed normal cardiac function. Transient ventricular fibrillation was observed during resuscitation, but he soon developed cardiac arrest. Cardiac pulmonary resuscitation was unsuccessfully performed, and he died of sudden circulatory failure.

Correspondence: Daiichiro Hasegawa, MD, PhD, Department of Hematology and Oncology, Kobe Children's Hospital, 1-1-1, Suma, Kobe, Japan. Email: hasegawa_kch@hp.pref.hyogo.jp

Received 25 August 2007; revised 8 April 2008; accepted 9 April 2008.
doi: 10.1111/j.1442-200X.2009.02925.x

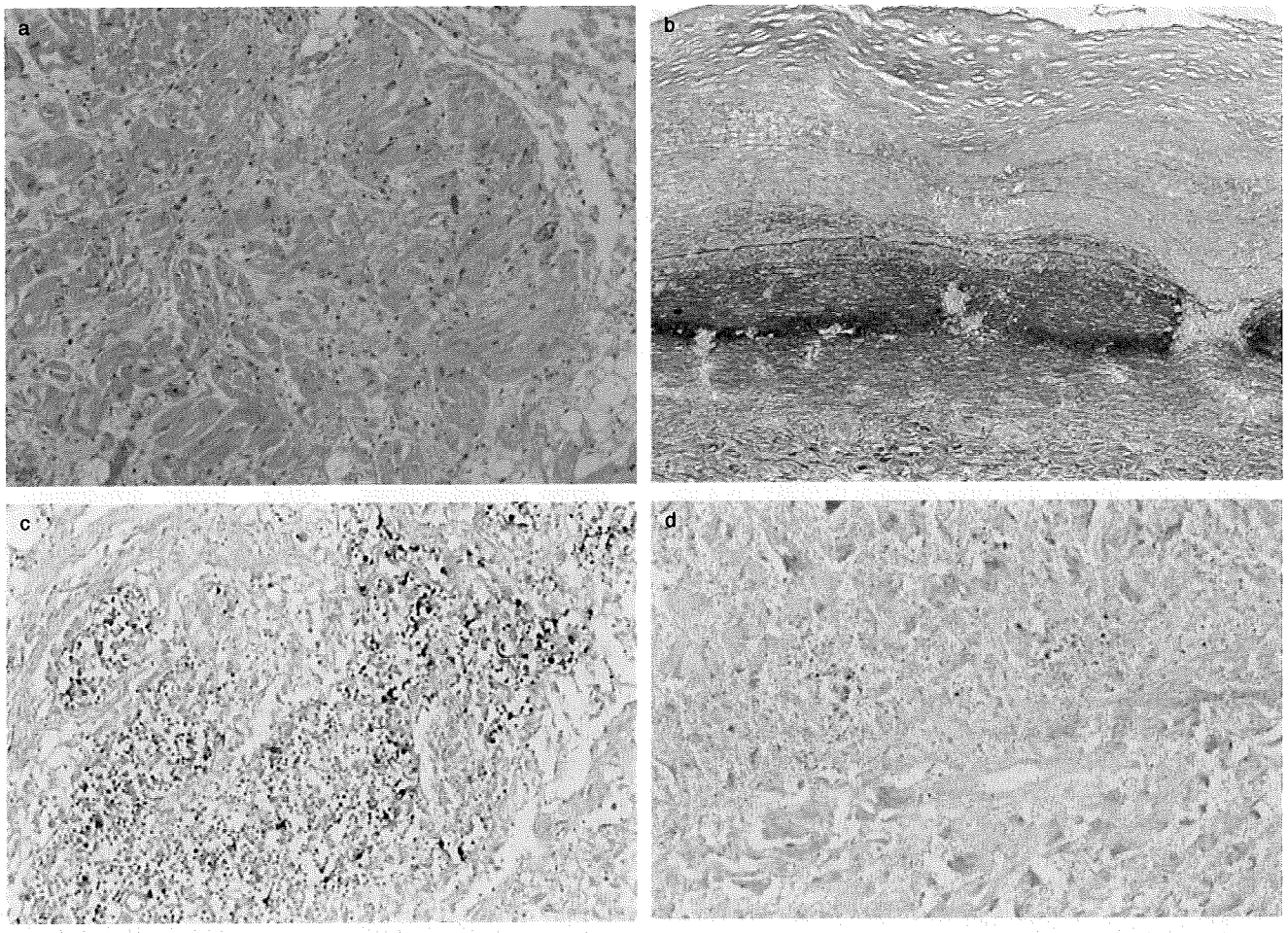

Fig. 1 (a) Histopathology showed degeneration of specialized cardiac muscle (HE), and mesoarteritis characterized by moth-eaten-appearing destruction of the medial elastic laminae, with (b) lymphocyte infiltration around the vasa vasorum and severe intimal thickening (EVG). (c) *In situ* hybridization demonstrated the presence of EBV-RNA (EBER-1) in the nuclei of lymphocytes in lymph nodes and (d) degenerated cardiac muscles.

At autopsy, histopathology showed not only EBV-associated hemophagocytic syndrome, but also degeneration of specialized cardiac muscle (Fig. 1a), mesoarteritis characterized by moth-eaten-appearing destruction of the medial elastic laminae (Fig. 1b), with $CD4^+$T lymphocyte infiltration around the vasa vasorum and severe intimal thickening. *In situ* hybridization demonstrated the presence of EBV-RNA (EBER-1) in the nuclei of lymphocytes in lymph nodes (Fig. 1c), around the vessels and degenerated cardiac muscles (Fig. 1d). Hemorrhagic tendency associated with disseminated intravascular coagulation syndrome was also noted at autopsy, although fatal intracranial hemorrhage and myocardial infarction were not documented. These findings suggested that hemophagocytic syndrome and degeneration of specialized cardiac muscles might have caused the fatal arrhythmia, considered to be associated with the EBV infection.

Discussion

In the current case, coronary artery dilatations and large-vessel arteritis were noted at autopsy. Arteritis has been reported in patients with CAEBV.[6] Coronary arteries and large vessels are often involved, and the presence of arteritis associated with EBV infection led to poor prognoses in those reported patients.[6-8] The vulnerability of systemic vessels caused by severe arteritis might be involved in the poor response to cardiopulmonary resuscitation. *In situ* hybridization showed that EBV-infected lymphocytes were associated with mesoarteritis, characterized by moth-eaten-appearing destruction of the medial elastic laminae and severe intimal thickening. Taken together, a comparatively high load of EBV-DNA persisting prior to transplantation might have been one of the factors promoting arteritis in this patient.

To our knowledge this is the first case reported in the literature in which the degeneration of specialized cardiac muscle was documented at autopsy in a patient with CAEBV. Transient ventricular fibrillation was also detected on ECG during cardiopulmonary resuscitation. The degeneration of specialized cardiac muscle might lead to fatal arrhythmia and acute circulatory failure. *In situ* hybridization also showed that EBER-positive

cells were scattered around cardiac muscle, suggesting that persistent EBV infection was involved in the degeneration of specialized cardiac muscle, Atrioventricular block has also been reported in EBV myocarditis.[9] These findings suggest that prolonged EBV infection could lead to the degeneration of specialized cardiac muscle over a long period.

Allogeneic HSCT has been reported to offer a good prognosis for those with CAEBV.[2,3] A national survey, however, performed in Japan found a high risk of HSCT-related mortality.[5] Recently, successful treatment of CAEBV infection using reduced-intensity stem cell transplantation (RIST) with fludarabine and melphalan with or without anti-thymocyte globulin (ATG) has been reported,[10,11] which could control CAEBV by reconstituting host immunity against EBV. Regimen-related toxicity is expected to be more effectively alleviated using a reduced intensity conditioning regimen for transplantation than by conventional myeloablative conditioning in those with an impaired residual function of organs. In contrast, it is well known that the risk of EBV-related complications after transplantation might increase with the additional use of ATG in non-myeloablative conditioning.[12] In the current case we adapted fludarabine-based, reduced-intensity conditioning with ATG for transplantation, because it was predicted that the residual cardiac function might be partly impaired by coronary giant aneurysms. The additional use of ATG, however, in fludarabine-based conditioning might have been involved in the development of hemophagocytic syndrome during preconditioning for transplantation, although it was uncertain whether the serum sickness induced by the use of ATG was associated with the degeneration of cardiac muscle. To answer the many remaining questions, such as the best transplantation method for CAEBV, the optimal timing of transplantation, and the most effective conditioning regimen, a multicenter-based clinical trial is needed.

References

1 Cohen JI. Epstein-Barr virus infection. *N. Engl. J. Med.* 2000; **343**: 481–92.
2 Okano M. Overview and problematic standpoints of severe chronic active Epstein-Barr virus infection syndrome. *Crit. Rev. Oncol. Hematol.* 2002; **44**: 273–82.
3 Fujii N, Takenaka K, Hiraki A *et al.* Allogeneic peripheral blood stem cell transplantation for the treatment of chronic active Epstein-Barr virus infection. *Bone Marrow Transplant.* 2000; **26**: 805–8.
4 Okamura T, Hatsukawa Y, Arai H, Inoue M, Kawa K. Blood stem-cell transplantation for chronic active Epstein-Barr virus with lymphoproliferation. *Lancet* 2000; **356**: 223–4.
5 Kimura H, Hoshino Y, Kanegane H *et al.* Clinical and virologic characteristics of chronic active Epstein-Barr virus infection. *Blood* 2001; **98**: 280–86.
6 Murakami K, Ohsawa M, Hu SX, Kanno H, Aozasa K, Nose M. Large-vessel arteritis associated with chronic active Epstein-Barr virus infection. *Arthritis Rheum.* 1998; **41**: 369–73.
7 Kikuta H, Sakiyama Y, Matsumoto S *et al.* Detection of Epstein-Barr virus DNA in cardiac and aortic tissues from chronic, active Epstein-Barr virus infection associated with Kawasaki disease-like coronary artery aneurysms. *J. Pediatr.* 1993; **123**: 90–92.
8 Kimura H, Morishima T, Kanegane H *et al.* Prognostic factors for chronic active Epstein-Barr virus infection. *J. Infect. Dis.* 2003; **187**: 527–33.
9 Reitman MJ, Zirin HJ, DeAngelis CJ. Complete heart block in Epstein-Barr myocarditis. *Pediatrics* 1978; **62**: 847–9.
10 Sakata N, Sato E, Sawada A, Yasui M, Inoue M, Kawa K. Chronic active Epstein-Barr virus infection treated with reduced intensity stem cell transplantation. *Rinsho Ketsueki* 2004; **45**: 393–6.
11 Sawada A, Inoue M, Koyama M *et al.* Complete elimination of endogenous EBV after allogeneic UCBT. *Rinsho Ketsueki* 2007; **48**: 1111.
12 Brunstein CG, Weisdorf DJ, DeFor T *et al.* Marked increased risk of Epstein-Barr virus-related complications with the addition of antithymocyte globulin to a nonmyeloablative conditioning prior to unrelated umbilical cord blood transplantation. *Blood* 2006; **108**: 2874–80.

Congenital upper thoracic spondyloptosis with multiple other associated anomalies

Banu Alicioglu, Mustafa Kemal Demir and Yavuz Durmus
Radiology Department, Trakya University School of Medicine, Edirne, Turkey

Key words congenital abnormalities, diagnosis, scapula, spine, spondyloptosis.

Spondyloptosis indicates any slip greater than 100% of a vertebral body on another or an extreme degree of spondylolisthesis. It is rare and there are isolated case reports in the literature.[1,2] It frequently involves the L5–S1 level. It is attributed to congenital dysplasia of the articular process.[3]

Correspondence: Banu Alicioglu, MD, School of Medicine, Trakya University, 22030 Edirne, Turkey. Email: banualicioglu@trakya.edu.tr

Received 4 September 2007; revised 8 February 2008; accept 18 March 2008.
doi: 10.1111/j.1442-200X.2009.02926.x

Presented here is the case of an infant with severe spinal cord compression related to T2–3 spondyloptosis and multisegmental vertebral congenital anomaly. Multisystem anomalies such as Sprengle deformity, situs inversus totalis, and right renal agenesis were also demonstrated radiologically. To our knowledge this is a unique case of thoracic spondyloptosis.

Case report

A 9-month-old male infant presented with a significant delay in head holding. He was the result of the first pregnancy of young

Immunology
The Journal of cells, molecules, systems and technologies
British Society for immunology

IMMUNOLOGY ORIGINAL ARTICLE

Ex vivo expanded cord blood CD4 T lymphocytes exhibit a distinct expression profile of cytokine-related genes from those of peripheral blood origin

Yoshitaka Miyagawa,[1] Nobutaka Kiyokawa,[1] Nakaba Ochiai,[2,3] Ken-Ichi Imadome,[4] Yasuomi Horiuchi,[1] Keiko Onda,[1] Misako Yajima,[4] Hiroyuki Nakamura,[4] Yohko U. Katagiri,[1] Hajime Okita,[1] Tomohiro Morio,[2,5] Norio Shimizu,[2,6] Junichiro Fujimoto[7] and Shigeyoshi Fujiwara,[4]

[1]*Department of Developmental Biology, National Research Institute for Child Health and Development, Setagaya-ku,* [2]*Center for Cell Therapy, Tokyo Medical and Dental University Medical Hospital, Bunkyo-ku, Tokyo,* [3]*Lymphotec Inc., Koto-ku, Tokyo,* [4]*Department of Infectious Diseases, National Research Institute for Child Health and Development, Setagaya-ku, Tokyo,* [5]*Department of Pediatrics and Developmental Biology, Graduate School of Medicine, Tokyo Medical and Dental University, Bunkyo-ku, Tokyo,* [6]*Department of Virology, Division of Medical Science, Medical Research Institute, Tokyo Medical and Dental University, Bunkyo-ku, Tokyo, and* [7]*Vice Director General, National Research Institute for Child Health and Development, Setagaya-ku, Tokyo, Japan*

Summary

With an increase in the importance of umbilical cord blood (CB) as an alternative source of haematopoietic progenitors for allogenic transplantation, donor lymphocyte infusion (DLI) with donor CB-derived activated $CD4^+$ T cells in the unrelated CB transplantation setting is expected to be of increased usefulness as a direct approach for improving post-transplant immune function. To clarify the characteristics of activated $CD4^+$ T cells derived from CB, we investigated their mRNA expression profiles and compared them with those of peripheral blood (PB)-derived activated $CD4^+$ T cells. Based on the results of a DNA microarray analysis and quantitative real-time reverse transcriptase–polymerase chain reaction (RT-PCR), a relatively high level of forkhead box protein 3 (Foxp3) gene expression and a relatively low level of interleukin (IL)-17 gene expression were revealed to be significant features of the gene expression profile of CB-derived activated $CD4^+$ T cells. Flow cytometric analysis further revealed protein expression of Foxp3 in a portion of CB-derived activated $CD4^+$ T cells. The low level of retinoic acid receptor-related orphan receptor γ isoform t (RORγt) gene expression in CB-derived activated $CD4^+$ T cells was speculated to be responsible for the low level of IL-17 gene expression. Our data indicate a difference in gene expression between $CD4^+$ T cells from CB and those from PB. The findings of Foxp3 expression, a characteristic of regulatory T cells, and a low level of IL-17 gene expression suggest that CB-derived $CD4^+$ T cells may be a more appropriate source for DLI.

Keywords: CD4; cord blood; donor lymphocyte infusion; forkhead box protein 3; interleukin 17; T cell

doi:10.1111/j.1365-2567.2009.03122.x
Received 1 September 2008; revised 30 March 2009; accepted 15 April 2009.
Correspondence: N. Kiyokawa, MD, PhD, Department of Developmental Biology, National Research Institute for Child Health and Development, 2-10-1, Okura, Setagaya-ku, Tokyo 157-8535, Japan.
Email: nkiyokawa@nch.go.jp
Senior author: Nobutaka Kiyokawa

Abbreviations: BIM, BCL2-like 11; CB, cord blood; CTLA-4, cytotoxic T-lymphocyte antigen-4; CDKN, cyclin-dependent kinase inhibitor; DLI, donor lymphocyte infusion; Foxp3, forkhead box protein 3; GAPDH, glyceraldehyde-3-phosphate dehydrogenase; GM-CSF, granulocyte–macrophage colony-stimulating factor; GVHD, graft-versus-host disease; GVL, graft-versus-leukaemia; HSCT, haematopoietic stem cell transplantation; ICOS, inducible T-cell co-stimulator; IFNG, interferon γ; IL, interleukin; PB, peripheral blood; RORγt, retinoic acid receptor-related orphan receptor γ isoform t; RT, reverse transcriptase; TCR, T-cell receptor; Th, T helper cell; Treg, regulatory T cell.

Introduction

Donor lymphocyte infusion (DLI) is a direct and useful approach for improving post-transplant immune function. DLI has been shown to exert a graft-versus-leukaemia (GVL) effect and has emerged as an effective strategy for the treatment of patients with leukaemia, especially chronic myelogenous leukaemia, who have relapsed after unrelated haematopoietic stem cell transplantation (HSCT).[1] In addition, DLI has been successfully used for some life-threatening viral infections, including Epstein–Barr virus and cytomegalovirus infections after HSCT.[2]

Although DLI frequently results in significant acute and/or chronic graft-versus-host disease (GVHD), several groups have demonstrated that depletion of CD8 T cells from DLIs efficiently reduces the incidence and severity of GVHD while maintaining GVL activity.[3,4] Therefore, selective CD4 DLI is expected to provide an effective and low-toxicity therapeutic strategy for improving post-transplant immune function. Actually, selective CD4 DLI based on a recently established method for *ex vivo* T-cell expansion using anti-CD3 monoclonal antibody and interleukin (IL)-2 is now becoming established as a routine therapeutic means of resolving post-transplant immunological problems in Japan.[5]

The importance of umbilical cord blood (CB) as an alternative source of haematopoietic progenitors for allogenic transplantation, mainly in patients lacking a human leucocyte antigen (HLA)-matched marrow donor, has increased in recent years. Because of the naïve nature of CB lymphocytes, the incidence and severity of GVHD are reduced in comparison with the allogenic transplant setting. In addition, CB is rich in primitive $CD16^-$ $CD56^+$ natural killer (NK) cells, which possess significant proliferative and cytotoxic capacities, and so have a substantial GVL effect.[6]

In contrast, a major disadvantage of CB transplantation is the low yield of stem cells, resulting in higher rates of engraftment failure and slower engraftment compared with bone marrow transplantation. In addition, it was generally thought to be difficult to perform DLI after CB transplantation using donor peripheral blood (PB), with the exception of transplantations from siblings. However, the above-described method for the *ex vivo* expansion of activated T cells can produce a sufficient amount of cells for therapy using the CB cell residues in an infused bag, which has solved this problem and made it possible to perform DLI with donor CB-derived activated $CD4^+$ T cells in the unrelated CB transplantation setting.[5] It has also been reported that CB-derived T cells can be expanded *ex vivo* while retaining the naïve and/or central memory phenotype and polyclonal T-cell receptor (TCR) diversity,[7] and thus potential utilization for adoptive cellular immunotherapy post-CB transplantation has been suggested.[8]

There are functional differences between CB and PB lymphocytes, although the details remain unclear. In an attempt to clarify the differences in characteristics between activated $CD4^+$ T cells derived from CB and those derived from PB, we investigated gene expression profiles. In this paper we present evidence that CB-derived $CD4^+$ T cells are distinct from PB-derived $CD4^+$ T cells in terms of gene expression.

Materials and methods

Cell culture and preparation

CB was distributed by the Tokyo Cord Blood Bank (Tokyo, Japan). The CB was originally collected and stored for stem cell transplantation. Stocks that were inappropriate for transplantation because they contained too few cells were distributed for research use with informed consent, with the permission of the ethics committee of the bank. In addition, all of the experiments in this study using distributed CB were performed with the approval of the local ethics committee. The mononuclear cells were isolated by Ficoll-Paque centrifugation and cultured in the presence of an anti-CD3 monoclonal antibody and interleukin (IL)-2 using TLY Culture Kit 25 (Lymphotec Inc., Tokyo, Japan) as described previously.[5] Although several different methods for T-cell stimulation have been reported, this method is currently being used clinically in Japan. Thus we selected this method in this study. After 14 days of culture, $CD4^+$ cells were isolated using a magnetic-activated cell sorting (MACS) system (Miltenyi Biotec, Bergisch Gladbach, Germany) according to the manufacturer's instructions. As a control, mononuclear cells isolated from the peripheral blood of healthy volunteers were similar examined.

Polymerase chain reaction (PCR)

Total RNA was extracted from cells using an RNeasy kit (Qiagen, Valencia, CA) and reverse-transcribed using a First-Strand cDNA synthesis kit (GE Healthcare Bio-Science Corp., Little Chalfont, Buckinghamshire, UK) according to the manufacturer's instructions. Using cDNA synthesized from 150 ng of total RNA as a template for one amplification, real-time reverse transcriptase (RT)-PCR was performed using SYBR® Green PCR master mix, TaqMan® Universal PCR master mix and TaqMan® gene expression assays (Applied Biosystems, Foster City, CA), and an inventoried assay carried out on an ABI PRISM® 7900HT sequence detection system (Applied Biosystems) according to the instructions provided. Either the glyceraldehyde-3-phosphate dehydrogenase (GAPDH) gene or the β-actin gene was used as an internal control for normalization. The sequences of gene-specific primers for real-time RT-PCR are listed in Table 1.

DNA microarray analysis

The microarray analysis was performed as previously described.[9] Total RNA isolated from cells was reverse-

Table 1. The sequences of gene-specific primers for reverse transcriptase–polymerase chain reaction (RT-PCR) and real-time RT-PCR used in this study

Primer	Sequence
IL-4 forward	CACAGGCACAAGCAGCTGAT
IL-4 reverse	CCTTCACAGGACAGGAATTCAAG
IL-6 forward	GTAGCCGCCCCACACAGA
IL-6 reverse	CCGTCGAGGATGTACCGAAT
IL-10 forward	GCCAAGCCTTGTCTGAGATGA
IL-10 reverse	CTTGATGTCTGGGTCTTGGTTCT
IL-17 forward	GACTCCTGGGAAGACCTCATTG
IL-17 reverse	TGTGATTCCTGCCTTCACTATGG
IL-17F forward	GCTTGACATTGGCATCATCAA
IL-17F reverse	GGAGCGGCTCTCGATGTTAC
IL-23 forward	GAGCCTTCTCTGCTCCCTGATAG
IL-23 reverse	AGTTGGCTGAGGCCCAGTAG
IL-23R forward	AACAACAGCTCGGCTTTGGTATA
IL-23R reverse	GGGACATTCAGCAGTGCAGTAC
IFNG forward	CATCCAAGTGATGGCTGAACTG
IFNG reverse	TCGAAACAGCATCTGACTCCTTT
GM-CSF forward	CAGCCCTGGAGCATGTG
GM-CSF reverse	CATCTCAGCAGCAGTGTCTCTAC[r]
RORγt forward	TGGGCATGTCCCGAGATG
RORγt reverse	GCAGGCTGTCCCTCTGCTT
STAT-3 forward	GGAGGAGGCATTCGGAAAGT
STAT-3 reverse	GCGCTACCTGGGTCAGCTT
FOXP3 forward	GAGAAGCTGAGTGCCATGCA
FOXP3 reverse	GCCACAGATGAAGCCTTGGT

IL, interleukin; *IFNG*, interferon γ; *FOXP3*, forkhead box protein 3; *GM-CSF*, granulocyte–macrophage colony-stimulating factor; *RORγt*, retinoic acid receptor-related orphan receptor γ isoform t; *STAT*, signal transducer and activator of transcription.

transcribed and labelled using One-Cycle Target Labeling and Control Reagents as instructed by the manufacturer (Affymetrix, Santa Clara, CA). The labelled probes were hybridized to a Human Genome U133 Plus 2·0 Array (Affymetrix). The arrays were used in a single experiment and analysed with GENECHIP operating software 1.2 (Affymetrix). Background subtraction and normalization were performed using GENESPRING GX 7.3 software (Agilent Technologies, Santa Clara, CA). The signal intensity was pre-normalized based on the positive control genes (GAPDH and β-actin) for all measurements on that chip. To account for differences in detection efficiency between spots, the pre-normalized signal intensity of each gene was normalized to the median of pre-normalized measurements for that gene. The data were filtered as follows. (i) Genes that were scored as absent in all samples were eliminated. (ii) Genes with a signal intensity of < 90 were eliminated. (iii) Genes that exhibited increased (fold-change > 2) or decreased (fold-change > 2) expression in CB-derived $CD4^+$ T cells compared with PB-derived $CD4^+$ T cells were selected by comparing the mean value of signal intensities in each condition.

Immunofluorescence study

After periods of cultivation, cells were collected and stained with fluorescence-labelled monoclonal antibodies and analysed by flow cytometry (FC500; Beckman/Coulter, Fullerton, CA). A four-colour immunofluorescence study was performed with a combination of fluorescein isothiocyanate (FITC)-conjugated anti-CD3, phycoerythrin (PE)-conjugated anti- forkhead box protein 3 (Foxp3), phycoerythrin-cyanine-5 (PC5)-conjugated anti-CD4 and PC7-conjugated anti-CD8 (Beckman/Coulter). After staining of cell surface antigens, cells were permeabilized with IntraPrep (Dako, Glostrup, Denmark) and intracellular antigen (Foxp3) was further stained.

Statistical analysis

The statistical analysis was performed using a Student's *t*-test and a *P*-value < 0·05 was considered to be statistically significant.

Results

Expression profiles of activated $CD4^+$ T cells derived from human CB and PB

To compare the gene expression patterns of CB-derived $CD4^+$ cells and PB-derived $CD4^+$ cells, we performed DNA microarray analysis using the Affymetrix Human Genome U133 Plus 2·0 Array. After background subtraction, comparison of the gene expression profiles of two independent CB-derived $CD4^+$ samples and PB-derived $CD4^+$ samples was performed using a gene cluster analysis. The genes differentially expressed (fold-change > 2) between the activated $CD4^+$ T cells derived from CB and those derived from PB were selected, and 396 probes were found to exhibit higher levels of expression in CB-derived $CD4^+$ samples while 131 probes exhibited higher levels in PB-derived $CD4^+$ samples. Parts of the data are summarized and presented in Fig. 1a and Tables 2–4.

Among these genes, those closely correlated to T-cell function and development were selected (Fig. 1b). The genes exhibiting higher levels of expression in CB-derived $CD4^+$ samples included those encoding cell cycle regulators, including cyclin-dependent kinase (CDKN)2A and 2B, transcriptional regulators and signal transduction factors (Tables 2 and 3). The genes for cytokines, chemokines and their receptors such as Interferon γ (IFNG), granulocyte-macrophage colony-stimulating factor (GM-CSF) and for T-cell transcriptional regulators (*FOXP3*) as well as the genes related to T-cell development including CD28, cytotoxic T lymphocyte antigen-4 (CTLA4) and inducible T-cell co-stimulator (ICOS) were also found among the genes exhibiting higher levels of expression in CB-derived $CD4^+$ samples (Fig. 1b). The factors reported

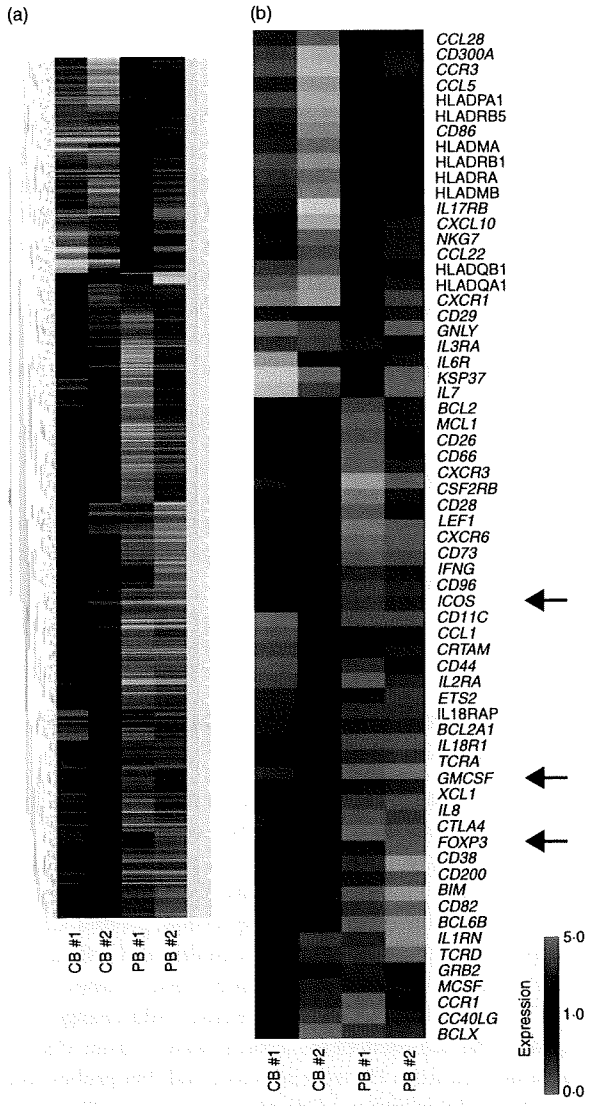

Figure 1. Comparison of the gene expression profiles of cord blood (CB)- and peripheral blood (PB)-derived $CD4^+$ T cells. Hierarchical clustering of results from a microarray analysis for CB- and PB-derived $CD4^+$ T cells is indicated. (a) A total of 529 genes characterizing $CD4^+$ T cells (396 genes for CB-derived $CD4^+$ T cells and 131 genes for PB-derived $CD4^+$ T cells) were used to create the gene tree. The gene list is presented in Tables 3 and 4. (b) Genes related to T-cell development (40 genes for CB-derived $CD4^+$ T cells and 26 genes for PB-derived $CD4^+$ T cells) are presented. The arrows indicate the expression pattern of T-cell lineage-specific genes including inducible T-cell co-stimulator (*ICOS*), granulocyte-macrophage colony-stimulating factor (*GM-CSF*) and forkhead box protein 3 (*FOXP3*).

to be essential for negative selection in $CD4^+$ $CD8^+$ thymocytes such as BCL2-like 11 (BIM)[10] as well as other apoptotic regulators were also found among the genes exhibiting higher expression levels in CB-derived $CD4^+$ samples.

The genes with a higher level of expression in the PB-derived $CD4^+$ T cells included those encoding transcriptional regulators, signal transduction factors, major histocompatibility complex (MHC) class II molecules (*HLADMA*, *HLADMB*, *HLADPA1*, *HLADQB1*, *HLADRA*, *HLADRB1* and *HLADRB5*), and cytokines, chemokines and their receptors (*IL-7*, *IL-17RB*), as well as genes that characterize the T-cell lineage (*CD29*, *CD86*) (Fig. 1b, Tables 2, 4).

Notably, microarray studies showed that the expression of several regulatory T cell (Treg)-related genes was significantly higher in the CB-derived T cells. Foxp3 is an important T-cell transcription factor and is considered to be a marker of Tregs. Cytotoxic T-lymphocyte antigen-4 (CTLA-4) and ICOS, which belong to the CD28 family of receptors and play a crucial role in the activation of T cells, were reported to be highly expressed in activated Tregs.[11,12] All of the above genes were expressed at higher levels in the CB-derived CD4 T cells (Fig. 1).

The microarray results for major genes related to the development of the T-cell lineage, including those not appeared in Fig. 1, are summarized in Table 2. As shown in Table 2, the expression of T-cell lineage master regulator genes, such as *TBX21*, *GATA3* and *MAF*, and T cell-related cytokines, such as *IL-4*, *IL-5*, *IL-13*, *IL-22* and *TGFB1*, revealed no significant difference between CB-derived $CD4^+$ cells and PB-derived $CD4^+$ cells. However, other T cell-related genes, including *IL-2*, *IL-6*, *IL-9*, *IL-10* and *IL-17*, were eliminated from the list in the course of background subtraction because the signal intensity of each gene was low (< 90 as raw data) in all of the samples.

Differences in the expression patterns of T-cell lineage-specific genes between CB-derived and PB-derived $CD4^+$ T cells

To further confirm the characteristic gene expression in CB- and PB-derived $CD4^+$ T cells, we performed a real-time RT-PCR analysis. Consistent with the microarray data, when the mRNA levels of the genes related to the T helper type 1 (Th1) and Th2 phenotypes were examined, higher levels of GM-CSF and IFNG were observed in CB-derived T cells, while IL-4 revealed no significant tendency (Fig. 2). We also examined IL-6 and IL-10 and no significant tendency was observed either in the expression of these genes (Fig. 2).

Next we examined the expression of the genes related to Tregs and observed a higher level of Foxp3, but lower levels of retinoic acid receptor-related orphan receptor γ isoform t (RORγt); and IL-17F, in CB-derived T cells (Fig. 3). In contrast, there was no significant tendency in the expression of genes encoding signal transducer and activator of transcription 3 (STAT-3), IL-23 and IL-23 receptors. In the case of the *IL-17* gene, clear amplifica-

Table 2. The microarray results for T-cell-related genes

			CB-1		CB-2		PB-1		PB-2	
Description	Gene	Gene ID	Normalized	Raw	Normalized	Raw	Normalized	Raw	Normalized	Raw
Master regulation										
Thl	*TBX21*	220684_at	1·1382915	305·7	0·7851455	247·1	1·045663	230·5	0·954337	261·4
Th2	*GATA3*	209602_s_at	1·471558	1204	0·7742825	742·1	1·0740323	721·1	0·9259675	772·5
	GATA3	209603_at	1·265932	416·5	0·53335179	205·7	1·0535141	284·5	0·9464856	317·6
	GATA3	209604_s_at	1·350573	5300	0·6415387	2950	1·0573606	3406	0·9426395	3773
	MAF	206363_at	0·7447395	672·7	0·8744312	925·6	1·1255689	834·5	1·2704437	1170
	MAF	209348_s_at	1·0320604	2078	0·8329663	1965	0·9679398	1600	1·8301903	3758
	MAF	229327_s_at	0·9099149	569·7	0·6089576	446·8	1·090085	560·2	1·4076804	898·9
Treg	*FOXP3*	221334_s_at	1·8893701	100·6	1·4199468	88·6	0·4988136	21·8	0·5800531	31·5
	FOXP3	224211_at	1·6205869	152·3	1·4101433	155·3	0·5898568	45·5	0·2347433	22·5
Cytokines										
Thl	*IFNG*	210354_at	1·4801383	2000	1·9182948	3037	0·457517	507·4	0·5198616	716·4
	GM-CSF	210229_s_at	1·2802086	1293	2·6726868	3163	0·6906437	572·5	0·7197912	741·4
Th2	*IL-4*	207538_at	2·0291064	687·2	0·3361219	133·4	0·9317174	259	1·0682826	369
	IL-4	207539_s_at	2·8263247	965	0·3561467	142·5	0·8481774	237·7	1·1518226	401·1
	IL-5	207952_at	1·3380713	810	0·0610382	43·3	1·0097023	501·7	0·9902797	611·4
	IL-13	207844_at	3·9835246	1712	0·8117443	408·8	1·1453367	404	0·8691162	452·9
Treg	*TGFB1*	203085_s_at	1·5166419	774·9	0·9012154	539·6	1·0987847	460·8	0·8546632	374·6
Others	*IL-22*	222974_at	0·1272062	5·2	4·325279	207·2	0·5632869	18·9	1·4367131	59·9
Surface molecules										
Treg	*CTLA4*	231794_at	1·3871489	336·9	1·2560804	357·5	0·7439196	148·3	0·4444751	110·1
	CTLA4	236341_at	1·2573498	905·7	1·6210791	1368	0·6800935	402·1	0·7426501	545·6
Others	*IL-2RA*	206341_at	1·5216751	3569	1·2715347	3494	0·7284654	1402	0·6569936	1571
	IL-2RA	211269_s_at	1·1563299	4436	1·3173387	5923	0·8436702	2657	0·560745	2194
	ICOS	210439_at	1·378036	619·8	1·343834	708·3	0·567216	209·4	0·656166	301
	CD28	211856_x_at	1·3887135	144·9	1·2905376	157·8	0·3292731	28·2	0·7094624	75·5
	CD28	211861_x_at	1·350062	183·3	1·4109998	224·5	0·4863549	54·2	0·649938	90

The microarray results for major genes related to the development of the T-cell lineage are summarized. The normalized and raw data for four samples are indicated for each gene. Those for which differential expression was found between cord blood (CB)- and peripheral blood (PB)-derived $CD4^+$ T cells in a gene cluster analysis (fold-change > 2) are highlighted in grey. Genes exhibiting low signal intensity (< 90 as raw data) in all of the four samples were eliminated from the list beforehand in the process of background subtraction, and thus do not appeared in this table.

CTLA-4, cytotoxic T-lymphocyte antigen-4; *FOXP3*, forkhead box protein 3; GATA, GATA family of zinc finger trancription factors; *GM-CSF*, granulocyte–macrophage colony-stimulating factor; ICOS, inducible T-cell co-stimulator; IFNG, interferon γ; *IL*, interleukin; MAF, macrophage-activating factor; TBX21, T-box protein 21; TGFB1, transforming growth factor, beta 1; Th1, T helper type 1; Treg, regulatory T cell.

tion was detected in PB-derived T cells whereas no amplification was observed in the samples of CB-derived T cells (data not shown).

To further investigate whether increased expression of the *FOXP3* gene is a general feature of CB-derived $CD4^+$ T cells, we tested four samples of CB-derived $CD4^+$ T cells by real-time RT-PCR analysis and compared the results with those for equivalent numbers of PB-derived samples. As shown in Fig. 4, two CB-derived samples (CB 4 and 5, at 2 weeks) revealed significantly increased gene expression of *FOXP3* when compared with PB-derived samples, whereas the remaining two samples (CB 3 and 6; termed 'additional' samples below) did not. We also tested *FOXP3* gene expression at an earlier time-point in the same samples and observed no significant increase of *FOXP3* gene expression in CB-derived $CD4^+$ T cells at 1 week (Fig. 4). When the data were analysed statistically, expression of the *FOXP3* gene was found to be significantly higher in CB-derived $CD4^+$ T cells in comparison with equivalent PB-derived $CD4^+$ T cells at both 1 week ($P < 0{\cdot}05$) and 2 weeks ($P < 0{\cdot}05$) (Fig. 4).

Next we assessed the expression of the Foxp3 protein in CB-derived $CD4^+$ T cells. When the same samples as described above were examined by flow cytometry using a specific antibody, the Foxp3 protein was certainly detected in a portion of cells in all of four CB-derived samples while not detected in any of the PB-derived samples tested (Fig. 5). Inconsistent with the results of real-time RT-PCR, expression level of Foxp3 proteins was higher in CB-derived $CD4^+$ T cells at 1 week than at 2 weeks.